Neurotherapeutics (2021) 18:1113–1126
https://doi.org/10.1007/s13311-021-01025-6

ORIGINAL ARTICLE

Specific Expression of Glial-Derived Neurotrophic Factor in Muscles as Gene Therapy Strategy for Amyotrophic Lateral Sclerosis

Guillem Mòdol-Caballero[1,2,3] · Belén García-Lareu[1,3,4] · Mireia Herrando-Grabulosa[1,2,3] · Sergi Verdés[1,4,5] · Rubén López-Vales[1,2,3] · Gemma Pagès[4] · Miguel Chillón[1,4,5,6] · Xavier Navarro[1,2,3] · Assumpció Bosch[1,3,4,5]

Accepted: 5 February 2021 / Published online: 30 March 2021
© The American Society for Experimental NeuroTherapeutics, Inc. 2021

Abstract

Glial cell line–derived neurotrophic factor (GDNF) is a powerful neuroprotective growth factor. However, systemic or intrathecal administration of GDNF is associated with side effects. Here, we aimed to avoid this by restricting the transgene expression to the skeletal muscle by gene therapy. To specifically target most skeletal muscles in the mouse model of amyotrophic lateral sclerosis (ALS), SOD1^{G93A} transgenic mice were intravenously injected with adeno-associated vectors coding for GDNF under the control of the desmin promoter. Treated and control SOD1^{G93A} mice were evaluated by rotarod and nerve conduction tests from 8 to 20 weeks of age, and then histological and molecular analyses were performed. Muscle-specific GDNF expression delayed the progression of the disease in SOD1^{G93A} female and male mice by preserving the neuromuscular function; increasing the number of innervated neuromuscular junctions, the survival of spinal motoneurons; and reducing glial reactivity in treated SOD1^{G93A} mice. These beneficial actions are attributed to a paracrine protective mechanism from the muscle to the motoneurons by GDNF. Importantly, no adverse secondary effects were detected. These results highlight the potential of muscle GDNF-targeted expression for ALS therapy.

Key Words GDNF · Amyotrophic lateral sclerosis · Motoneuron · Gene therapy · AAV · Neuromuscular junction

Introduction

Amyotrophic lateral sclerosis (ALS) is a neurodegenerative disease without effective therapy currently available. Loss of spinal and cortical motoneurons (MN) leads to progressive muscular weakness, paralysis, and death in a few years [1, 2]. Most ALS cases are sporadic, with no genetic association. About 10% of ALS cases are familial, associated with different genes, including Cu/Zn superoxide dismutase 1 (*SOD1*), hexanucleotide repeat expansions in chromosome 9 open reading frame 72 (*C9ORF72*), and TAR DNA-binding protein 43 (*TARDP*) among others [1–3]. Several physiopathological mechanisms have been identified, mostly using ALS murine models, in the disease process, including glutamatergic excitotoxicity, mitochondrial dysfunction, oxidative stress, altered axonal transport, proteasome dysfunction, synaptic deficits, neuroinflammation, and microglial activation, all leading to selective MN degeneration [2, 4, 5]. The multiple events that contribute to MN death make particularly difficult developing effective therapies for this disease. After decades of research in pre-clinical models and numerous clinical trials, only two drugs are approved by the FDA, Riluzole, an inhibitor of synaptic glutamate release, and

---

Guillem Mòdol-Caballero, Belén García-Lareu, and Mireia Herrando-Grabulosa contributed equally to this work.

✉ Xavier Navarro
xavier.navarro@uab.cat

✉ Assumpció Bosch
assumpcio.bosch@uab.cat

[1] Institute of Neurosciences, Universitat Autònoma de Barcelona, 08193 Bellaterra, Spain

[2] Department Cell Biology, Physiology and Immunology, Universitat Autònoma de Barcelona, Barcelona, Spain

[3] Centro de Investigación Biomédica en Red Sobre Enfermedades Neurodegenerativas (CIBERNED), Instituto de Salud Carlos III, Madrid, Spain

[4] Department of Biochemistry and Molecular Biology, Universitat Autònoma de Barcelona, Barcelona, Spain

[5] Unitat Mixta UAB-VHIR, Vall D'Hebron Institut de Recerca (VHIR), Barcelona, Spain

[6] Institut Català de Recerca I Estudis Avançats (ICREA), Barcelona, Spain

Edaravone, a free radical scavenger, although they only prolong ALS patients' life by 2–3 months [6–8].

The most successful therapeutic strategy in the transgenic SOD1 mice, the most used ALS animal model, is the targeted knockdown of the mutant SOD1 gene, which has been accomplished through different strategies. One is by direct administration of antisense oligonucleotides into the CSF in rodent models [9], which is currently being tested in clinical trials [10]. Another is the use of AAV vectors driving RNA inhibition against SOD1, which significantly prolonged the life span in mutant SOD1 mice even if administered after the onset of the disease [11] and that were efficient also in control non-human primates [12]. And finally, viral vectors have been also used to deliver gene editing tools to the same mouse model with significant delay in the disease onset and survival [13, 14]. However, only a very small percentage of ALS patients contain mutations to the *SOD1* gene. Thus, alternative strategies should be approached in order to find a general treatment for most ALS patients. It has been proposed that treatments acting simultaneously on several implicated mechanisms and targeting different cell types involved in neurodegeneration, will likely be more effective to improve the course of ALS. The progressive death of MN in ALS is preceded by failure of neuromuscular junctions (NMJ) and axonal retraction [15, 16], dependent upon defects in the interaction of motor axons with terminal Schwann cells and skeletal muscle fibers. Thus, for an effective therapy, it seems necessary to simultaneously enhance MN survival, maintain the integrity of the NMJ, and promote reinnervation of the muscles denervated during the initial phases of the disease [17].

In this regard, neurotrophic factors expressed by different cell types provide a balanced support essential for MN development and survival [18–21]. Thus, several trophic factors that are involved in MN biology, such as insulin-like growth factor (IGF-1), vascular endothelial growth factor (VEGF), ciliary neurotrophic factor (CNTF), and glial cell line-derived neurotrophic factor (GDNF), have been suggested as potential therapies for ALS [22–26]. Notably, the use of viral vectors encoding growth factors has been one of the most effective approaches to delay the progression of MN degeneration among the preclinical therapeutic assays conducted.

We focused this work on GDNF, a growth factor with neuroprotective effects on both dopamine and MN in vitro [27–29] and in vivo in different models of disease [21, 30–33]. When administered into the spinal cord, GDNF preserved spinal MN in ALS rats, although NMJ innervation and lifespan were not improved, compared with untreated animals. Local muscle injection of an adeno-associated viral vector (AAV) encoding for GDNF in ALS mice or transplantation of mesenchymal stem cells genetically engineered to overexpress GDNF in ALS rats provided some beneficial functional effects [23, 34–37]. On the other hand, systemic delivery of GDNF has secondary effects in the brain and causes body weight loss [38]. Indeed, clinical trials using GDNF have failed so far due to problems with pharmacokinetics and dose-limiting toxicity after CSF delivery (for review see Luz et al. [39]). Therefore, optimal delivery methods need to be explored. As a proof of concept, double transgenic animals expressing GDNF in the muscle and mutant SOD1 showed improved preservation of NMJ and spinal MN, probably due to retrograde transport, since GDNF does not cross the blood brain barrier. Thus, effective gene therapy for ALS would require distribution of the therapeutic gene throughout all the muscles in the body, only achievable by systemic delivery of a gene transfer vector capable of specifically transducing skeletal muscles. Here we report MN survival and maintenance of muscle innervation in SOD1^{G93A} mice by selectively upregulating the expression of GDNF in skeletal muscle using an AAV under the regulation of the human desmin promoter.

Methods

Transgenic Mice

Transgenic mice with the G93A human SOD1 mutation (C57bl6-Tg[SOD1-G93A]1Gur) were obtained from the Jackson Laboratory (Bar Harbor, ME, USA). Hemizygotes C57bl6 SOD1^{G93A} males were obtained by crossing with C57bl6 females. The offspring was identified by PCR of DNA extracted from tail tissue. Experimental procedures were approved by the Ethics Committee of the Universitat Autònoma de Barcelona. The following experimental groups of mice were used: SOD1^{G93A} injected with AAV8-hDesGDNF or AAV8-Mock, WT littermates treated with AAV8-hDesGDNF or AAV8-Mock (n = 15–19/condition, 7–10 per each gender). To compensate the experimental groups, we allocated the animals according to weight and litter of origin. Animals were weighted every 4 weeks to monitor their overall health condition.

Virus Production and Injection

To isolate mouse GDNF cDNA sequence, total mRNA was obtained from an injured sciatic nerve of a WT adult mouse. Specific mRNA for mouse GDNF was amplified by RT-PCR using the following primers containing BamHI and NheI restriction sites: GDNF Fwd 5′-GGATCCGACGCTAGCTGGATGGGATTCGGGCCAC-3′ and GDNF Rev 5′-GGATCCGACGCTAGCGGGTCAGATACATCCACACC-3′. GDNF cDNA was confirmed by sequencing.

Mouse GDNF cDNA and firefly luciferase were cloned between AAV2 ITRs under the regulation of the human desmin promoter (provided by G Lemke, Salk Institute, La Jolla, CA, USA). AAV8 and AAV9 viral stocks were produced by the Viral Production Unit of UAB-VHIR (www.viralvector.eu) by triple transfection into HEK293-AAV cells of the expression plasmids, Rep8Cap2 or Rep9Cap2 plasmids containing AAV genes (provided by J.M. Wilson, University of Pennsylvania, Philadelphia, USA), and pXX6 plasmid containing adenoviral genes [40] needed as helper virus. AAV particles were purified by iodixanol gradient. Titration was evaluated by picogreen (Invitrogen) quantification and calculated as viral genomes per milliliter (vg/ml). Control serotype-matching AAV empty vectors (mock) were used as control.

For intravenous administration, 1.8×10^{14} vg/kg of AAV8-GDNF or AAV8-Mock in a total volume of 250 µl suspension were injected in the tail vein of 5-week-old mice.

In Vivo Imaging

Optical imaging studies were carried out with an IVIS Spectrum (Perkin Elmer, MA, USA) at the VHIR animal facility. Animals were anesthetized with isofluorane and shaved to minimize light absorbance. D-luciferine was intraperitoneally injected at 150 mg/kg in 0.2 ml. Images were obtained for 5 min after luciferine administration using the following parameters: FOV 22 mm, binning 8, F-stop 1. Light radiance was quantified in photons/sec/cm^2/steradian.

Electrophysiological Tests

Motor nerve conduction tests were performed every 4 weeks from 8 to 20 weeks of age. The sciatic nerve was stimulated by single pulses (Grass S88 stimulator) delivered through needle electrodes placed at the sciatic notch. The evoked compound muscle action potential (CMAP) was recorded from gastrocnemius (GM) and plantar interossei (PL) muscles with microneedle electrodes [16]. Electromyographic signals were amplified and displayed on a digital oscilloscope (Tektronix 450S), for measuring the amplitude and the latency of the CMAP.

Motor unit number estimation (MUNE) was performed using the incremental technique [16, 41]. The sciatic nerve was stimulated with single pulses of increasing intensity producing quantal increases in CMAP amplitude. Increments higher than 50 µV were considered due to recruitment of a new motor unit. The mean amplitude of single motor units was calculated from at least 15 consistent increases. The MUNE was calculated as the ratio of the CMAP maximal amplitude and the mean amplitude of motor unit action potentials.

Motor evoked potentials were evaluated to assess central motor pathways. Electrical stimuli of supramaximal intensity were delivered with needle electrodes placed subcutaneously over the skull overlaying the sensorimotor cortex, and the MEPs recorded from GM muscle using microneedle electrodes [16].

Locomotion Tests

Motor coordination, strength, and balance were evaluated by means of the Rotarod test in treated and untreated SOD1^{G93A} animals ($n = 6$/group). Each mouse was placed three times in the rotarod turning at a constant speed of 14 rpm and the longest time until falling recorded. A maximum time of 180 s was set. The test was performed every other week from 8 to 20 weeks of age. Clinical disease onset for each mouse was determined as the first week when the maintenance time was lower than 180 s.

Histology

At 20 weeks of age, mice were transcardially perfused with 4% paraformaldehyde in PBS and the lumbar spinal cord, tibial nerve, and gastrocnemius muscles were harvested. For spinal MN evaluation, spinal cords were postfixed during 4 h, cryopreserved in 30% sucrose in PBS, and 40 µm transverse sections cut using a cryotome (Leica). One every two slides of each animal were stained with cresyl violet. Motoneurons were identified by their localization in the ventral horn and following strict size and morphological criteria [16].

For NMJ labeling, the GM muscles were cryopreserved in 30% sucrose in PBS and 60-µm longitudinal sections were serially cut with a cryotome and collected in sequential series of 10. Sections were blocked with PBS-Triton-FBS and incubated 48 h at 4 °C with primary antibodies anti-synaptophysin (1:500, AB130436, Abcam), anti-neurofilament 200 (NF200, 1:1000, AB5539, Millipore), and anti-S100β (1:1, 22,520, Immunostar). After washes, sections were incubated overnight with Alexa 594-conjugated secondary antibody (1:200; Life Science) and Alexa 488 conjugated α-bungarotoxin (1:200, B-13422, Life technologies). The proportion of innervated endplates was determined by classifying each endplate as either occupied (when presynaptic terminals overly the endplate) or vacant (no presynaptic label in contact with the endplate). At least 4 fields totaling > 100 endplates were analyzed per muscle. For collateral sprouting, the number of sprouts per endplate was counted as the neurofilament-positive projections from pre-synaptic terminal or pre-terminal nodes on confocal z projections. For analysis, we considered both the total number of sprouts and the proportion of occupied end plates that were innervated by a collateral sprout.

For glial cell immunolabeling, transverse sections of L4-L5 cord segments were blocked with PBS-0.3%Triton-10%Normal Donkey serum and 20 mM glycine and incubated 24 h at 4 °C with primary antibodies anti-ionized calcium binding adapter molecule 1 (Iba-1, 1:1000; 019-19741, Wako) for microglia. Overnight incubation with Alexa 488-conjugated secondary antibody (1:200; A21206, Invitrogen) and DAPI (1:2000; D9563-10MG, Sigma) counterstaining were used. Images were obtained with a fluorescence microscope (Nikon Eclipse NI, Japan) and a region of interest centered in the ventral horn was selected to measure the integrated density of Iba-1 labeling using ImageJ software (NIH, Bethesda, MD).

Nucleic Acid Extraction and Real-Time PCR

DNA was extracted from different tissues with 0.1 mg/ml of proteinase K (Roche Diagnostics), followed by phenol/chloroform extraction. Real-time primers for cyclophilin B, as housekeeping gene, or desmin-luciferase construct, where the forward primer is located in the desmin promoter sequence and the reverse primer in the transgene sequence, are listed in Supplementary Table 1. Viral genome copies per cell were calculated using a standard curve generated from known amounts of plasmid DNA containing the Desmin-luciferase sequence or a cyclophilin PCR product purified by Geneclean (Q-Biogene) in 10 ng/ml salmon sperm DNA (Sigma) and assuming that 1 mg of mouse genomic DNA contains 3×10^5 haploid genomes [42].

For RNA extraction, 1000 µl of Qiazol (Qiagen) were added, and tissue homogenized for 6 min with Tyssue Lyser LT (Qiagen) at 50 Hz twice. Then, samples were purified with chloroform, precipitated with isopropanol, washed with 70% ethanol, and resuspended in 20 µl RNAse free water. The RNA concentration was measured using a NanoDrop ND-1000 (Thermo Scientific).

One microgram of RNA was reverse-transcribed using 10 µmol/l DTT, 200 U M-MuLV reverse transcriptase (New England BioLabs), 10 U RNase Out Ribonuclease Inhibitor (Invitrogen), 1 µmol/l oligo(dT), and 1 µmol/l of random hexamers (BioLabs). The reverse transcription cycle conditions were 25 °C for 10 min, 42 °C for 1 h, and 72 °C for 10 min. We analyzed the mRNA expression of GDNF, RET, Nrg1tIII, and ErbB4, by means of specific primer sets (Supplementary Table 1). Mouse 36B4 was used to normalize the expression levels of the different genes.

Gene-specific mRNA analysis was performed by SYBR-green real-time PCR using the MyiQ5 real-time PCR detection system (Bio-Rad Laboratories). The thermal cycling conditions comprised 5-min polymerase activation at 95 °C, 45 cycles of 15 s at 95 °C, 30 s at 60ºC, 30 s at 72 °C, and 5 s at 65 °C to 95 °C (increasing 0.5 °C every 5 s). Fluorescence detection was performed at the end of the PCR extension, and melting curves were analyzed by monitoring the fluorescence of the SYBR Green signal.

Protein Extraction and Detection

Another part of the GM muscle and of the spinal cord were prepared for protein extraction and homogenized in modified RIPA buffer (50 mM Tris–HCl pH 7.5, 1% Triton X-100, 0.5% sodium deoxycholate, 0.2% SDS, 100 mM NaCl, 1 mM EDTA) adding 10 µl/ml of Protease Inhibitor cocktail (Sigma) and PhosphoSTOP phosphatase inhibitor cocktail (Roche). After clearance, protein concentration was determined by PierceTM BCA Protein Assay Kit (Thermo Scientific).

For Western blots, 20–60 µg of protein of each sample were loaded in SDS-poliacrylamide gels. The transfer buffer was 25 mM trizma-base, 192 mM glycine, 20% (v/v) methanol, and pH 8.4. The membranes were blocked with 5% BSA in PBS plus 0.1% Tween-20 for 1 h, and then incubated with primary antibodies overnight. The primary antibodies used were rabbit anti-GDNF (1:200, sc-328, Santa Cruz Biotechnology), goat anti-Ret (1:100, #AF482, R&D Systems), rabbit anti-phospho Akt T308 (1:500; #9275 Cell Signaling), rabbit anti-Akt (1:1000; #9272 Cell Signaling), rabbit anti-pErk 1/2 (1:500, #9101, Cell Signaling), rabbit anti-total Erk 1/2 (1:1000, #9102, Cell Signaling), rabbit anti-GAPDH (1:1000; #2118, Cell Signaling), and rabbit anti-actin (1:1000, #A2066, Sigma). Horseradish peroxidase–coupled secondary antibody (swine anti-rabbit or rabbit anti-goat, 1:10,000; #P0399 or # P0160, Dako) and Westar Eta C Ultra 2.0 ECL substrate (CYANAGEN) were added. Image density was quantified with Image LabTM software (Bio-Rad). Samples of a minimum of 3 animals per group were used, and at least 3 different blots were quantified for each marker.

Measurement of GDNF concentration in plasma, spinal cord, liver, and skeletal muscle homogenates was performed by a specific ELISA according to the manufacturer's instructions (Aviva Systems Biology, OKCD05717). Plasma samples were diluted to one-third, and values for the different tissues were represented as ng GDNF/mg total protein ($n = 3$ per experimental condition, samples in duplicate).

For ex vivo luciferase activity quantification, protein extracts were obtained by lysing the tissues according to manufacturer's instructions (Pierce Firefly Luciferase Flash Assay kit, ThermoFisher Scientific). Luminescence was read in VICTOR3 (PerkinElmer). Transduction efficiency was expressed as values of luminescence per microgram protein.

Data Analysis

All experiments were performed by researchers blinded for the different treatments of each mouse group, and random allocation of animals in groups taking into account weight and litter. Data are expressed as mean ± SEM. Electrophysiological and locomotion test results were statistically analyzed using one-way or repeated measurements ANOVA with Tukey post hoc test. For MUNE and MEP electrophysiological results, Student's *t* test was applied. For clinical disease, onset Log-rank (Mantel-Cox) test was applied. Histological and molecular biology data were analyzed using *t*-Student, one- or 2-way ANOVA with Tukey or Holm-Sídák post hoc tests.

Results

Vector Biodistribution in Wild Type and ALS Mice

With the aim to prove specific delivery to skeletal muscles in ALS mice, we used the human desmin promoter driving the expression of firefly luciferase. We tested whether AAV vectors were able to transduce the affected muscles in the SOD1^{G93A} mouse independently of disease status. Thus, we assessed biodistribution in the mice at 10 weeks of age, when the disease started to be evident, and at 15 weeks, when it has progressed to a clear phenotype. Via tail vein, we systemically administered 4×10^{13} viral genomes (vg)/kg of body weight in a volume of 250 µl of two different serotypes of AAV vectors, AAV8 and AAV9, both described as efficient in transducing muscles from the circulation ($n = 5$

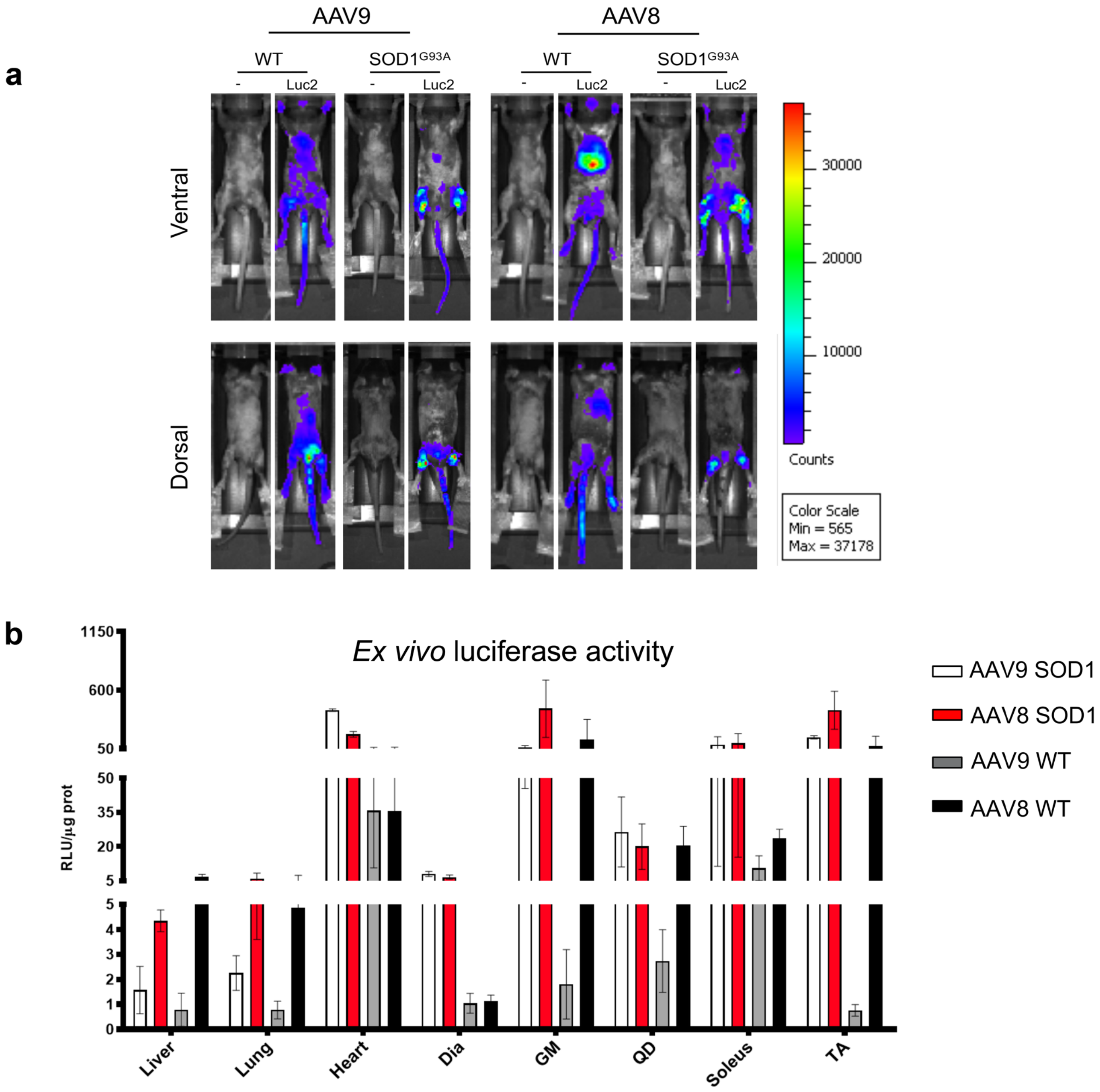

Fig. 1 In vivo imaging assay of viral bio-distribution. (**a**) In vivo luciferase biodistribution driven by human desmin promoter in SOD1^{G93A} and WT mice. Intravenous administration of AAV8 and AAV9 coding for hDes-Luciferase efficiently transduced most skeletal muscles in mice, independently of genotype, gender and stage of disease. (**b**) Ex vivo luciferase activity normalized by µg of protein showing high levels of expression in different skeletal muscles and heart, while liver and lung transduction are near background levels. GM gastrocnemius, QD quadriceps, TA tibialis anterior, dia diaphragm. Sex and genotypes were pooled

per genotype and vector, including 2 males and 3 females per group). Animals were analyzed 5 weeks later by in vivo imaging of luciferase activity (Fig. 1a). We further confirmed the in vivo results by ex vivo luciferase activity in isolated tissues (Fig. 1b). Independently of gender, mouse genotype, or AAV serotype, we obtained high transduction in all skeletal muscles analyzed: gastrocnemius, quadriceps, tibialis anterior, and soleus, and in the heart (Fig. 1b) and tongue (*data not shown*). On the contrary, liver, lung, spinal cord, and brain showed near to background levels (Fig. 1b), although most viral particles ended in the liver, as shown by the number of vg/cell in the same tissues (Supplementary Fig. 1).

Intravenous Delivery of Desmin-GDNF Vector Induces Expression in Skeletal Muscles

Mouse GDNF cDNA was retrotranscribed from mouse sciatic nerve and cloned into AAV2 backbone (Supplementary Fig. 2A). Its bioactivity was demonstrated by its ability to induce neurite outgrowth 10 days after transfection of PC12 cell line, widely used as a model for neural differentiation (Supplementary Fig. 2B top). Quantitative PCR confirmed expression of GDNF (Supplementary Fig. 2C). The secretion of GDNF was verified by transfecting of HEK293 cells, the supernatant collected 4 days later and used to visualize neurite outgrowth of PC12 cells. Medium from mock-transfected cells was used as negative control (Supplementary Fig. 2B bottom).

The AAV8 serotype was chosen for the therapeutic assay due to a slightly better infection of this vector in the SOD1^{G93A} mice. We intravenously administered a suspension of GDNF-Desmin-AAV8 (Fig. 2a) and mock-Desmin-AAV8 vectors at 1.8×10^{14} vg/kg in 250 µl to 5-week-old SOD1^{G93A} mice of C57/bl6 background, short before the disease onset, estimated at 6–7 weeks, based on electrophysiological data (Mancuso et al., 2012). We increased the viral titers by almost 0.5 log, based on our recently published data in this model demonstrating the need of higher titers to achieve therapeutic effects from the muscle [43]. The experimental design is detailed in Fig. 2b. By quantitative PCR (Fig. 2c), immunohistochemistry (Fig. 2d) and Western blot (Fig. 2f, g) we found an increase in GDNF expression in gastrocnemius (GM) and in tibialis anterior (TA) muscles of treated animals. While we found significantly increased levels of GDNF protein quantified by enzyme-linked immunosorbent assay (ELISA) in TA muscles of treated than control mice (Fig. 2e), we did not detect differences in plasma, liver, and spinal cord (Supplementary Table 2). This confirms the tissue specificity of the desmin promoter, already demonstrated in Fig. 1, and suggests that GDNF is poorly secreted from transduced muscles, probably due to the low secretory activity of this tissue compared to liver [44]. Consequently with overexpression of GDNF, we observed a slower progression of the locomotion decline in treated SOD1^{G93A} mice as evaluated by the rotarod test (Fig. 2h; 6 mice/group; $p < 0.05$), as well as a delayed clinical disease onset (Fig. 2i) compared to control SOD1^{G93A} ($p = 0.05$).

Fig. 2 GDNF overexpression in skeletal muscles after intravenous ▶ administration of AAVhDes-GDNF. (**a**) Diagram of the viral construct. (**b**) Experimental timeline: AAV8 vector containing the GDNF under the human desmin promoter was intravenously administered to 5 week-old WT and SOD^{G93A} mice. AAV8 Mock virus was used as control. Progression of the disease was analyzed by electrophysiological and rotarod tests. Animals were euthanized at 20 weeks of age. (**c**) At the endpoint, GDNF expression was quantified by means of mRNA by quantitative RT-PCR in gastrocnemius muscles (GM), by immunohistochemistry (**d**) in tibialis anterior muscles (TA; $n = 3$/group); by ELISA (**e**) in both muscles or by Western blot from whole GM muscle protein extracts (**f**) and normalized by relative amount of actin densitometry in WT mock treated mice (**g**). *Statistical significance by 2-way ANOVA compared to SOD^{G93A} mock mice (*$p < 0.05$; **$p < 0.01$; ***$p < 0.001$); $^{\#}$compared to WT mock mice ($^{\#\#\#}p < 0.001$). Data are mean ± SEM. (**h**) GDNF overexpression produced a delay in the rotarod performance decline of treated SOD1^{G93A} mice compared to Mock treated mice ($n = 6$ mice per group; *$p < 0.05$). (**i**) Clinical onset of disease was also delayed ($p = 0.05$)

GDNF Overexpression in Skeletal Muscles Preserves Neuromuscular Function in SOD1^{G93A} Mice

Animals treated with the therapeutic virus maintained constant body weight through the study (Fig. 3a), without the reduction in body weight shown by non-treated SOD1^{G93A} mice during the last 4 weeks of follow-up. Animal fur and other signs of welfare were checked every other week, and no changes were reported through the experiment except those attributed to the disease. Thus, no negative effect of systemic overexpression of GDNF was detected in WT or SOD1^{G93A} animals, contrary to what was previously reported with systemic AAV-GDNF administration in mice [38], as well as in intracerebroventricular delivery in human patients and non-human primates [39].

Neuromuscular function was analyzed by electrophysiological tests in the hindlimbs of SOD1^{G93A} mice. No statistically significant differences were detected between genders (see also [45]); thus, we pooled results from male and female mice. The data showed significant preservation of the plantar (PL) and GM compound muscle action potential (CMAP) amplitude from weeks 12 and 8, respectively, in treated SOD1^{G93A} mice when compared to control SOD1^{G93A} mice (Fig. 3 b and c). The higher CMAP amplitude of hindlimb muscles was explained by an increase of the mean amplitude and the number of surviving motor units in treated animals (Fig. 3d, e). Motor unit number estimation (MUNE) provides quantitative information about the number of functional motor units in a muscle,

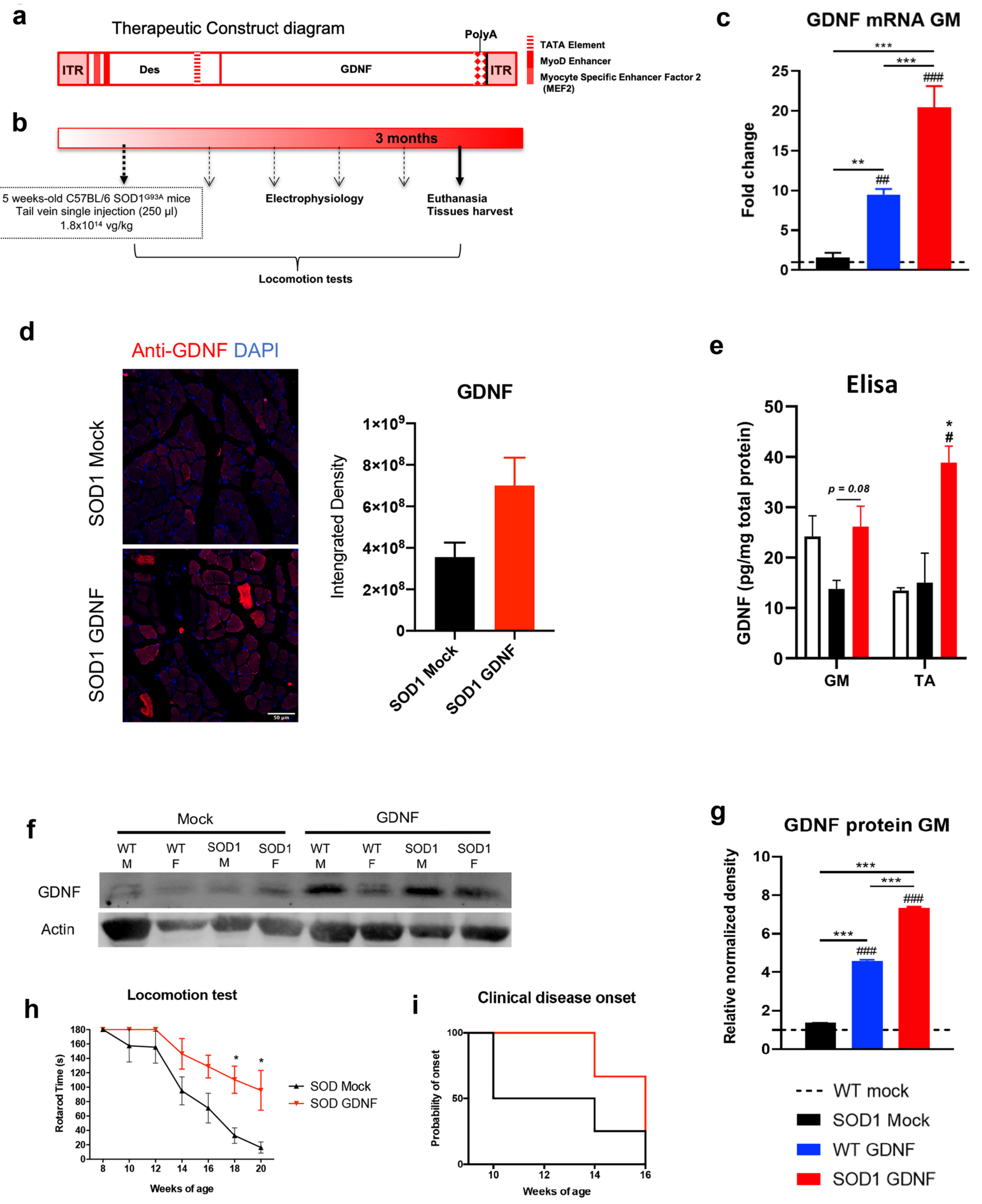

and it is crucial for the evaluation of progressive motor axonal loss in ALS [46, 47]. The distribution of motor units of the GM muscle grouped by amplitude of their action potential showed a higher number in most of the intervals (Fig. 3f). The amplitude of the motor evoked potentials (MEP) recorded in the GM muscles was also significantly

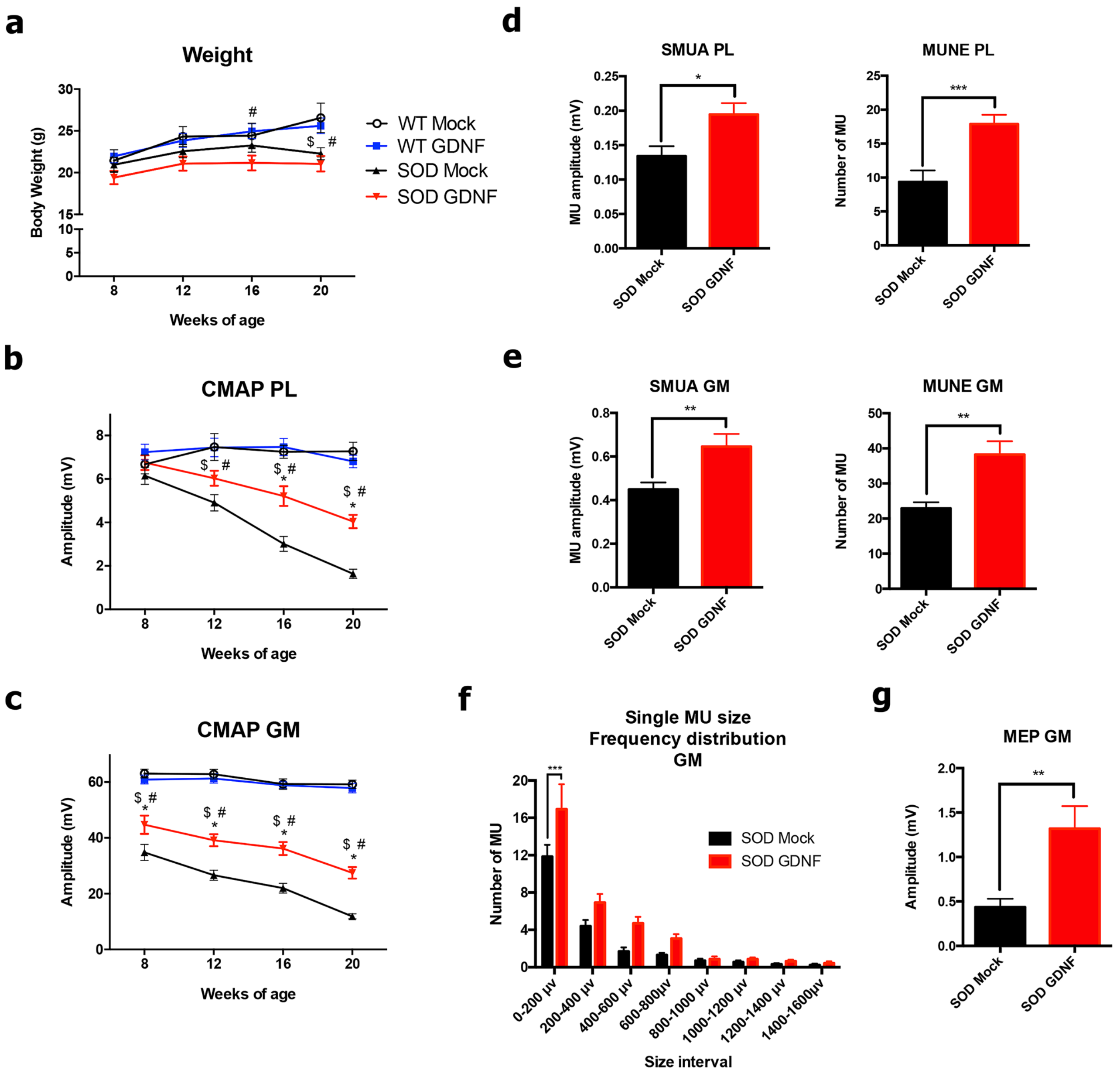

Fig. 3 GDNF overexpression promotes motor functional improvement of the SOD1^{G93A} mice. **a** Body weight gain was stable during follow-up in the three mouse groups but not for the SOD^{G93A} mock group which declined from 20 weeks of age. Electrophysiological tests show that AAV8-GDNF administration produced a significant preservation of the CMAP amplitude of PL (**b**), and GM (**c**) muscles in the SOD1^{G93A} mice along time. Electrophysiological estimation of motor unit number (MUNE) and mean amplitude of single motor unit potential (SMUA) of the PL (**d**) and GM (**e**) muscles shows preservation of more motor units and of larger size, confirmed by the amplitude frequency distribution (**f**). (**g**) GDNF treatment increased the amplitude of the MEPs at 20 weeks of age compared to SOD Mock mice. Data are mean ± SEM. Sexes were pooled: $n = 13$ WT Mock, 16 WT GDNF, 16 SOD Mock, 18 SOD GDNF, $^{*}p < 0.05$ vs SOD Mock mice; $^{\#}p < 0.05$ vs WT mice; $^{\$}p < 0.05$ vs WT Mock

higher in treated SOD1^{G93A} mice (Fig. 3g), indicating also higher preservation of central motor pathways. Moreover, motor function of ALS mice correlated with the levels of GDNF detected by both mRNA and ELISA in skeletal muscles (Supplementary Fig. 3A, B), as well as with the GM muscle mass of treated mice, which was close to that of WT animals, while untreated SOD1^{G93A} mice showed marked muscle atrophy (data not shown).

GDNF Overexpression in Skeletal Muscles Promoted Motor Functional Improvement in Treated SOD1^{G93A} Mice

Muscle-driven GDNF overexpression promoted a higher preservation of the number of occupied NMJ in the treated SOD1^{G93A} group (55.8 ± 7.1%; $p < 0.01$) compared to the mock SOD1^{G93A} group (33.2 ± 3.6%) (Fig. 4a), confirming the electrophysiological results of higher CMAP amplitude and MUNE values, although they were still lower than in WT animals.

GDNF cellular responses are mediated via a multicomponent receptor system consisting of a glycosyl-phosphatidylinositol-anchored membrane protein (GFRa-1) that binds GDNF on the cell surface and facilitates its interaction with the transmembrane tyrosine kinase RET receptor [48, 49] to activate intracellular signaling pathways via PI3K/AKT [50]. We found both Akt and Erk activation strongly downregulated in SOD1^{G93A} mice, whereas GDNF treatment completely restored Akt and Erk phosphorylation levels compared to the mock treated group (Fig. 4b, c).

On the other hand, GDNF and other neurotrophic factors increase neuregulin 1 (Nrg1) activity in cultured MN and also in embryonic spinal cord [51–53]. Since we recently reported that muscle-directed Nrg1 type I gene therapy promotes motor functional improvement in ALS mice ([43], we analyzed levels of Nrg1 and its receptors. We found that treatment with GDNF AAV vector significantly increased the expression of Nrg1 type I as well as expression of ErbB4 receptor, by more than 10 times ($p < 0.01$; Fig. 4d) in the GM muscle of treated SOD1^{G93A} and WT mice compared with mock treated mice. These results indicate a potent local paracrine action of the overexpressed GDNF in the skeletal muscle.

GDNF Overexpression in Skeletal Muscles Preserves Spinal MN and Reduces Neuroinflammation

GDNF production by muscle cells may be taken up by intramuscular motor axons and retrogradely transported to MN soma in the spinal cord. To confirm this hypothesis, we look for GDNF and its co-receptor expression. Whereas we did not find changes in GDNF levels in the spinal cord by either quantitative PCR (Fig. 5a), Western blot (Fig. 5b, c), or ELISA (Supplementary Table 2), we detected a significantly increased expression of GDNF RET receptor both as mRNA (Fig. 5a) and protein (Fig. 5d, e). On the other hand, GDNF treatment increased downstream signaling of Nrg1 type III and ErbB4 expression also in the spinal cord (Fig. 5a).

In agreement with molecular and functional results, we found a significant preservation of the number of MN in the ventral horn in treated SOD1^{G93A} mice (16.6 ± 1.0 mean number of MN per ventral horn) compared to the SOD1^{G93A} mock mice (9.3 ± 0.5; $p < 0.001$, $n = 7$–10 animals/group), although not reaching the values of WT mice ($p < 0.01$) (Fig. 5h, i). In addition, GDNF overexpression in muscles reduced also the inflammatory response in the lumbar spinal cord, with a significant decrease in the Iba1 immunoreactivity displayed by microglial cells compared to SOD1^{G93A} mock animals (Fig. 5c, d).

Altogether these data suggest that GDNF secreted from the muscles interacted through muscle innervation and mediated retrograde communication with spinal MN, activating some of their survival pathways and protecting them from excitotoxicity and inflammation.

Discussion

GDNF is a potent neurotrophic factor that protects the central and peripheral nervous system against degeneration, as demonstrated in several experimental models of neurodegenerative diseases, including Parkinson's disease and ALS [27, 54]. However, in the case of ALS, the wide distribution of affected MN, both in the brain cortex and along the brainstem and spinal cord, implies that an appropriate treatment requires global biodistribution of the therapeutic factor to target tissues. GDNF direct injection into the CNS, as well as systemic delivery through the circulation, was found deleterious in ALS and other preclinical and clinical assays [38, 39]. Here, by intravenous administration of an AAV vector under the regulation of the desmin promoter, we were able to reach most skeletal muscles and the heart, and to restrict its expression to the target tissue, which was enough to evade secondary effects, while achieving beneficial results in the ALS mice.

GDNF is one of the most potent survival factors for MN, and its mRNA was found increased in the initially denervated muscles of ALS and other MN disease patients but tended to decline in advanced stages of the pathology, suggesting that it represents a unspecific trophic response to ongoing denervation [55], but its effectiveness for treatment of MN diseases appears to depend significantly upon muscle specific expression. By cross-breeding SOD1^{G93A} mice with transgenic mice overexpressing GDNF either in skeletal muscle or in astrocytes, Li et al. [56] demonstrated that muscle-derived GDNF but not overexpression of GDNF in astrocytes resulted in neuroprotective effects. Similarly, intraspinal administration of lentiviral vector for GDNF did not prevent the loss of spinal MN and muscle denervation of the transgenic mice [57]. Approaches using stem cells genetically modified to release GDNF did not achieve functional improvement when transplanted into the spinal cord of SOD1^{G93A} rats [37], but delayed disease progression and increased the number of NMJ and MN at mid-stages of the disease when transplanted into several muscles [58].

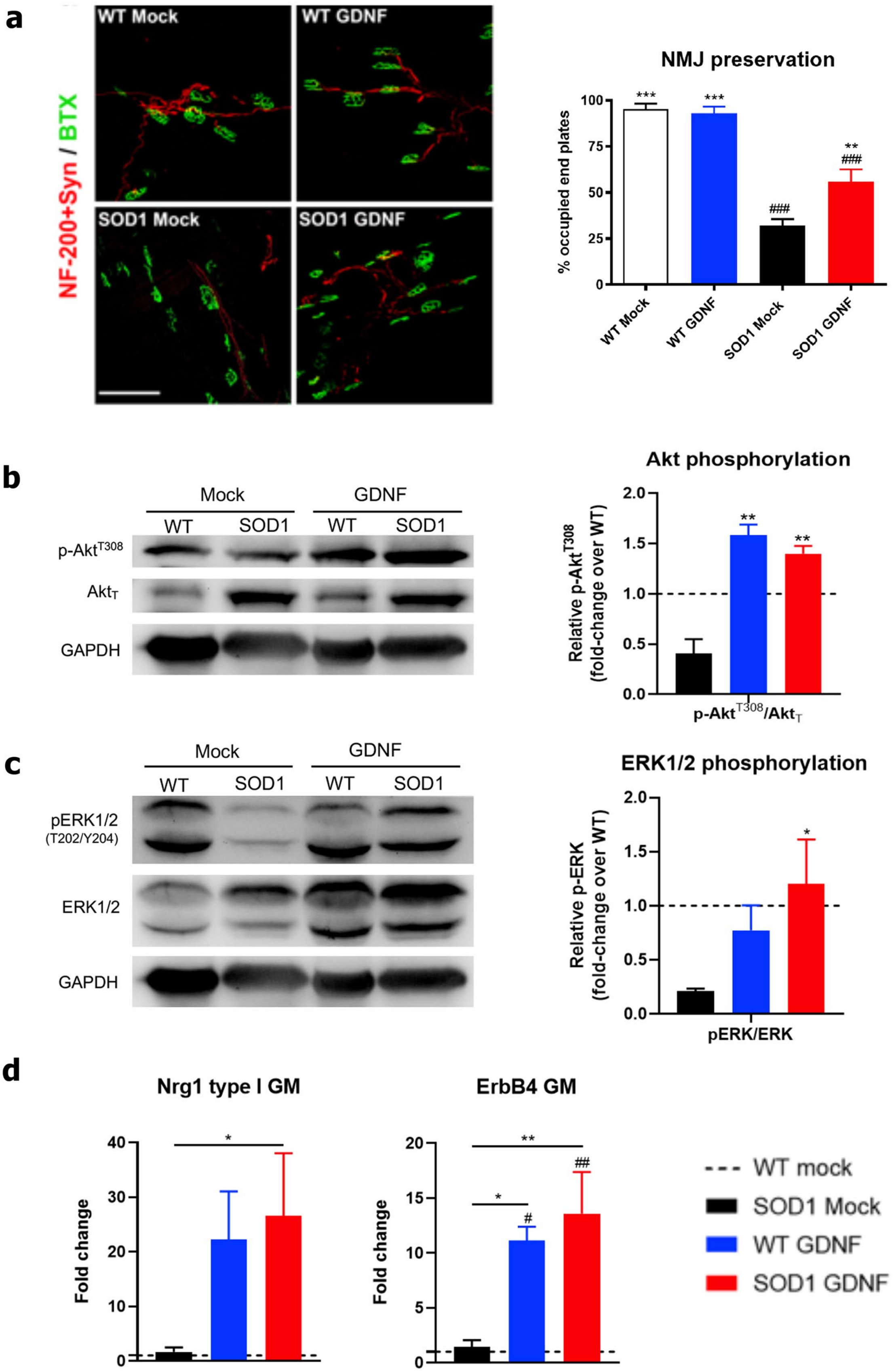
a
NF-200+Syn / BTX
WT Mock
WT GDNF
SOD1 Mock
SOD1 GDNF
NMJ preservation
% occupied end plates
0
25
50
75
100
***
***
###
**
###
WT Mock
WT GDNF
SOD1 Mock
SOD1 GDNF
b
Mock
GDNF
WT
SOD1
WT
SOD1
p-Akt^{T308}
Akt$_T$
GAPDH
Akt phosphorylation
Relative p-Akt^{T308} (fold-change over WT)
0.0
0.5
1.0
1.5
2.0
**
**
p-Akt^{T308}/Akt$_T$
c
Mock
GDNF
WT
SOD1
WT
SOD1
pERK1/2 (T202/Y204)
ERK1/2
GAPDH
ERK1/2 phosphorylation
Relative p-ERK (fold-change over WT)
0.0
0.5
1.0
1.5
2.0
*
pERK/ERK
d
Nrg1 type I GM
Fold change
0
10
20
30
40
*
ErbB4 GM
Fold change
0
5
10
15
20
**
*
#
##
WT mock
SOD1 Mock
WT GDNF
SOD1 GDNF

◀**Fig. 4** Increased GDNF signaling preserves NMJ and activates survival pathways in muscle of treated SOD^{G93A} mice. (**a**) Representative images of GM NMJ of WT and SOD1^{G93A} mice, treated with AAV8-GDNF or mock vector (scale bar = 100 µm). Histological analysis showed increased proportion of innervated NMJ in the treated SOD1^{G93A} mice compared to the Mock treated group (n = 5–7 WT, 5 WT GDNF, 7–9 SOD Mock, 9–10 SOD GDNF male-female mice per group, one-way ANOVA, $^{*}p < 0.05$ vs SOD Mock mice; $^{\#}p < 0.05$ vs WT mice). GDNF overexpression increased (**b**) Akt phosphorylation (Thr308) and (**c**) Erk1/2 activation in the muscle of SOD1^{G93A} treated animals, as demonstrated by Western blot. Quantifications show relative phosphorylation compared to total protein and normalized by GAPDH and are represented by fold-change compared to WT Mock animals (2-way ANOVA, $^{**}p < 0.01$ vs SOD Mock mice). (**d**) mRNA expression analysis of Nrg1 type I and ErbB4 receptor shows an upregulation upon GDNF overexpression in treated SOD1^{G93A} and WT mice compared to mock groups (2-way ANOVA, $^{*}p < 0.05$ or $^{**}p < 0.01$ vs SOD Mock mice; $^{\#}p < 0.05$ and $^{\#\#}p < 0.01$ vs WT mice)

In consequence, different approaches have been investigated to promote production of GDNF in skeletal muscles of SOD1^{G93A} mouse model. Single injection or electroporation of naked DNA in several muscles showed promising results [59, 60]. However, the neuroprotective effects of GDNF were more relevant when viral-mediated delivery into muscles was used. Adenovirus intramuscularly injected into neonatal mice resulted in GDNF expression not only in muscle cells but also in the spinal cord, due to retrograde axonal transport of the viral vector [34]. GDNF slightly delayed the onset of disease and the decline in motor functions, but GDNF expression declined over months of follow-up. Similarly, intramuscular delivery of GDNF by an AAV vector coding for a ubiquitous promoter led to stable expression of GDNF in a large number of myofibers and also in the anterior horn neurons, probably due to retrograde transport of the protein although retrograde transport of the vector cannot be discarded, since GDNF mRNA in the spinal cord was not checked [26, 35]. In the same study, injection of AAV-GDNF in the four-limbs of the mice delayed the progression of motor dysfunction and prolonged the life span in the treated ALS mice [26]. Our strategy has more translatable relevance as applying a single systemic injection of AAV encoding the GDNF under desmin promoter allowed to target a larger number of skeletal muscles in the body and showed comparatively higher improvement of the functional evolution and of the MN preservation.

With this targeted approach, we demonstrate that GDNF overexpression increases MN survival and reduces glial reactivity in the spinal cord of treated SOD1^{G93A} mice. We did not detect increased GDNF protein in spinal cord by either western blot or ELISA; thus, retrograde transport was not demonstrated. Nevertheless, activation of survival pathways in both skeletal muscle and spinal cord suggests a paracrine mechanism of protection from, at least, excitotoxicity and inflammation exerted by GDNF released from muscle cells, through induction of GDNF co-receptor in MN, and promoting other neurotrophic effects, particularly upregulating Nrg1 and ErbB4 expression in both muscle and spinal cord. Indeed, a positive feedback loop between Nrg1 and GDNF appears to exist; with increased Nrg1 type I in muscle and type III in spinal cord, both Nrg1 isoforms found altered in ALS mice and patients [17, 43, 61]. GDNF-induced increase of Nrg1 may have a dual beneficial effect. On one hand, Nrg1 type I expressed at the NMJ may act on terminal Schwann cells, which play a critical role for maintaining muscle innervation and motor axon survival [62], as we previously demonstrated by gene therapy [17, 43]. On the other hand, Nrg1 type III in the spinal cord may promote MN survival and decrease neuroinflammation [63]. Interestingly, short GDNF intrathecal treatment in aged rats restored GDNF and Nrg1 levels in muscles by ameliorating the neuromuscular dysfunction but did not inhibit the spinal cord microglial activation [64], probably because longer exposure to GDNF may be needed. According to our results, GDNF overexpression by targeting specifically skeletal muscles in other neuromuscular disturbances and in aging would be worth exploring.

In the SOD1^{G93A} mouse, motor clinical signs are usually observed around 11–13 weeks of age, but quantitative analysis demonstrated denervation of the NMJ and decline of motor nerve conduction results by 6–7 weeks [15, 45], followed later by progressive degeneration of motor axons and loss of MN cell bodies in the spinal cord. This pattern suggests a “dying-back” mechanism for MN disease in the SOD1^{G93A} mouse, where distal axonal degeneration occurs early during the disease, before neuronal degeneration and onset of symptoms [23]. According to this, GDNF applied at the NMJ but not in the soma compartment in microfluidic chambers of neuromuscular co-cultures facilitates axon growth and formation of active neuromuscular synapses [65]. Our data supports this hypothesis and provides a safe route for GDNF administration to ALS patients. Although this is only a proof-of-concept study, it suggests that treating the patients as early as possible, before the muscles start to be denervated and degenerating, may be necessary to achieve a therapeutic effect. Thus, identifying reliable biomarkers of the disease is crucial to facilitate earlier intervention and efficient treatments. For patients containing mutations in the *SOD1* gene, combining SOD1 inhibition with GDNF overexpression may be a possible therapy of choice.

In conclusion, we demonstrate here that muscle restricted GDNF expression at early stages of the disease is able to slow the progression of motor symptoms in SOD1^{G93A} animals by preserving the neuromuscular function, reducing NMJ denervation, protecting MN, and also contributing to revert the microglial inflammatory environment of the ALS mice.

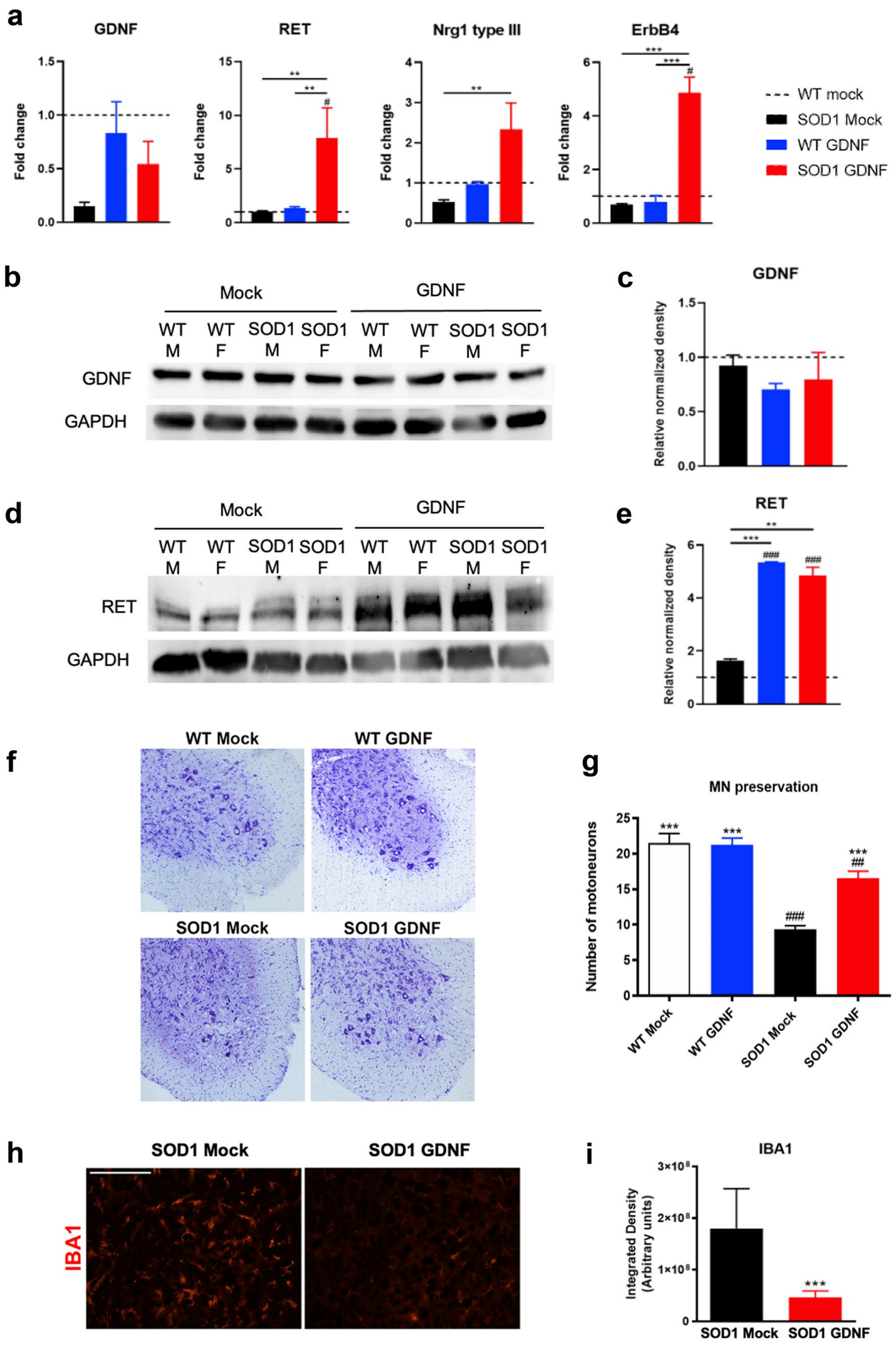
a
GDNF
RET
Nrg1 type III
ErbB4
Fold change
1.5
1.0
0.5
0.0
15
10
5
0
4
3
2
1
6
**
#
***
WT mock
SOD1 Mock
WT GDNF
SOD1 GDNF
b
Mock
GDNF
WT M
WT F
SOD1 M
SOD1 F
GDNF
GAPDH
c
GDNF
Relative normalized density
d
RET
GAPDH
e
RET
###
f
WT Mock
WT GDNF
SOD1 Mock
SOD1 GDNF
g
MN preservation
Number of motoneurons
25
20
15
10
5
0
***
##
###
WT Mock
WT GDNF
SOD1 Mock
SOD1 GDNF
h
SOD1 Mock
SOD1 GDNF
IBA1
i
IBA1
Integrated Density (Arbitrary units)
3×10⁸
2×10⁸
1×10⁸
0
***
SOD1 Mock
SOD1 GDNF

◀**Fig. 5** Overexpression of GDNF in the skeletal muscle promotes survival pathways in spinal cord leading to MN preservation and decreased neuroinflammation. (**a**) Real-time quantitative PCR of the spinal cord shows increased expression of GDNF coreceptor RET as well as Nrg1 type III and ErbB4 receptor without increasing GDNF expression in this tissue. Results are normalized by WT levels. (**b**) to (**e**) Western blot confirmed results shown in (**a**), with no differences in GDNF protein levels (**b**, quantified in **c**) but significant increase of RET coreceptor in treated animals (**d**, quantified in **e**). *Statistical significance by 2-way ANOVA compared to SOD mock animals (**$p < 0.01$; ***$p < 0.001$); #compared to WT mock animals (#$p<0.05$). (**f**) Representative images of L4 spinal cord of WT and SOD1^{G93A} mice, treated with AAV8-GDNF or mock vector (scale bar = 100 µm). (**g**) Histological analysis showed higher number of spinal MN (n = 5–7 WT Mock, 5–10 WT GDNF, 7–9 SOD Mock, 9–10 SOD GDNF male-female mice per group; one-way ANOVA, ***$p < 0.001$ vs SOD Mock mice; ##$p < 0.01$ and ###$p < 0.001$ vs WT mice). (**h**) Representative confocal images of microglia, labeled against Iba-1, in the spinal cord ventral horn of SOD1^{G93A} mice (scale bar = 100 µm). (**i**) Viral-mediated delivery of GDNF reduced microglia reactivity in treated SOD1^{G93A} mice (n = 7–9 SOD Mock, 9–10 SOD GDNF male-female mice, Student's T test, ***$p < 0.001$). Data are expressed as mean ± SEM

Supplementary Information The online version contains supplementary material available at https://doi.org/10.1007/s13311-021-01025-6.

Acknowledgements We thank Monica Espejo, Jessica Jaramillo, and Neus Hernández for unvaluable technical support.

Required Author Forms Disclosure forms provided by the authors are available with the online version of this article.

Funding This work was supported by grants TV3201428-10 of Fundació La Marato-TV3; RTI2018-096386-B-I00 of Ministerio de Ciencia, Innovación y Universidades (MCIU) and Agencia Estatal de Investigación (AEI) of Spain; TERCEL funds (RD16/0011/0014) from Instituto de Salud Carlos III of Spain; and European Union funds (ERDF/ESF, "Investing in your future"). SV is recipient of a predoctoral fellowship from Generalitat de Catalunya (2019 FI-B 00120).

References

1. Wijesekera LC, Leigh PN. Amyotrophic lateral sclerosis. Orphanet J Rare Dis 2009;4:3.
2. Hardiman O, Al-Chalabi A, Chio A et al. Amyotrophic lateral sclerosis. Nat Rev Dis Primers 2017;3:17085.
3. Renton AE, Chio A, Traynor BJ. State of play in amyotrophic lateral sclerosis genetics. Nat Neurosci 2014;17:17–23.
4. Pasinelli P, Brown RH. Molecular biology of amyotrophic lateral sclerosis: insights from genetics. Nat Rev Neurosci 2006;7:710–723.
5. Mancuso R, Navarro X. Amyotrophic lateral sclerosis: Current perspectives from basic research to the clinic. Prog Neurobiol 2015;133:1–26.
6. Doble A. The pharmacology and mechanism of action of riluzole. Neurology 1996;47:S233–241.
7. Ludolph AC, Jesse S. Evidence-based drug treatment in amyotrophic lateral sclerosis and upcoming clinical trials. Ther Adv Neurol Disord 2009;2:319–326.
8. Writing G, Edaravone ALSSG. Safety and efficacy of edaravone in well defined patients with amyotrophic lateral sclerosis: a randomised, double-blind, placebo-controlled trial. Lancet Neurol 2017;16:505–512.
9. McCampbell A, Cole T, Wegener AJ, et al. Antisense oligonucleotides extend survival and reverse decrement in muscle response in ALS models. J Clin Invest 2018;128:3558–3567.
10. Miller T, Cudkowicz M, Shaw PJ, et al. Phase 1-2 Trial of Antisense Oligonucleotide Tofersen for SOD1 ALS. N Engl J Med 2020;383:109–119.
11. Foust KD, Salazar DL, Likhite S, et al. Therapeutic AAV9-mediated suppression of mutant SOD1 slows disease progression and extends survival in models of inherited ALS. Mol Ther 2013;21:2148–2159.
12. Borel F, Gernoux G, Sun H, et al. Safe and effective superoxide dismutase 1 silencing using artificial microRNA in macaques. Sci Transl Med 2018;10.
13. Gaj T, Ojala DS, Ekman FK, et al. In vivo genome editing improves motor function and extends survival in a mouse model of ALS. Sci Adv 2017;3:eaar3952.
14. Lim CKW, Gapinske M, Brooks AK, et al. Treatment of a Mouse Model of ALS by In Vivo Base Editing. Mol Ther 2020;28:1177–1189.
15. Fischer LR, Culver DG, Tennant P, et al. Amyotrophic lateral sclerosis is a distal axonopathy: evidence in mice and man. Exp Neurol 2004;185:232–240.
16. Mancuso R, Santos-Nogueira E, Osta R, et al. Electrophysiological analysis of a murine model of motoneuron disease. Clin Neurophysiol 2011;122:1660–1670.
17. Mancuso R, Martinez-Muriana A, Leiva T, et al. Neuregulin-1 promotes functional improvement by enhancing collateral sprouting in SOD1(G93A) ALS mice and after partial muscle denervation. Neurobiol Dis 2016;95:168–178.
18. Bechade C, Mallecourt C, Sedel F, et al. Motoneuron-derived neurotrophin-3 is a survival factor for PAX2-expressing spinal interneurons. J Neurosci 2002;22:8779–8784.
19. Dugas JC, Mandemakers W, Rogers M, et al. A novel purification method for CNS projection neurons leads to the identification of brain vascular cells as a source of trophic support for corticospinal motor neurons. J Neurosci 2008;28:8294–8305.
20. Ikeda O, Murakami M, Ino H, et al. Acute up-regulation of brain-derived neurotrophic factor expression resulting from experimentally induced injury in the rat spinal cord. Acta Neuropathol 2001;102:239–245.
21. Tovar YRLB, Ramirez-Jarquin UN, Lazo-Gomez R, et al. Trophic factors as modulators of motor neuron physiology and survival: implications for ALS therapy. Front Cell Neurosci 2014;8:61.
22. Azzouz M, Ralph GS, Storkebaum E, et al. VEGF delivery with retrogradely transported lentivector prolongs survival in a mouse ALS model. Nature 2004;429:413–417.
23. Dadon-Nachum M, Melamed E, Offen D. The "dying-back" phenomenon of motor neurons in ALS. J Mol Neurosci 2011;43:470–477.
24. Dodge JC, Haidet AM, Yang W, et al. Delivery of AAV-IGF-1 to the CNS extends survival in ALS mice through modification of aberrant glial cell activity. Mol Ther 2008;16:1056–1064.
25. Kaspar BK, Llado J, Sherkat N, et al. Retrograde viral delivery of IGF-1 prolongs survival in a mouse ALS model. Science 2003;301:839–842.
26. Wang LJ, Lu YY, Muramatsu S, et al. Neuroprotective effects of glial cell line-derived neurotrophic factor mediated by an adeno-associated virus vector in a transgenic animal model of amyotrophic lateral sclerosis. J Neurosci 2002;22:6920–6928.
27. Henderson CE, Phillips HS, Pollock RA, et al. GDNF: a potent survival factor for motoneurons present in peripheral nerve and muscle. Science 1994;266:1062–1064.
28. Ibanez CF, Andressoo JO. Biology of GDNF and its receptors - Relevance for disorders of the central nervous system. Neurobiol Dis 2017;97:80–89.
29. Lin LF, Doherty DH, Lile JD, et al. GDNF: a glial cell line-derived neurotrophic factor for midbrain dopaminergic neurons. Science 1993;260:1130–1132.

30. Eggers R, Hendriks WT, Tannemaat MR, et al. Neuroregenerative effects of lentiviral vector-mediated GDNF expression in reimplanted ventral roots. Mol Cell Neurosci 2008;39:105–117.
31. Gash DM, Zhang Z, Ai Y, et al. Trophic factor distribution predicts functional recovery in parkinsonian monkeys. Ann Neurol 2005;58:224–233.
32. Rakowicz WP, Staples CS, Milbrandt J, et al. Glial cell line-derived neurotrophic factor promotes the survival of early postnatal spinal motor neurons in the lateral and medial motor columns in slice culture. J Neurosci 2002;22:3953–3962.
33. Zhang Z, Miyoshi Y, Lapchak PA, et al. Dose response to intraventricular glial cell line-derived neurotrophic factor administration in parkinsonian monkeys. J Pharmacol Exp Ther 1997;282:1396–1401.
34. Acsadi G, Anguelov RA, Yang H, et al. Increased survival and function of SOD1 mice after glial cell-derived neurotrophic factor gene therapy. Hum Gene Ther 2002;13:1047–1059.
35. Lu YY, Wang LJ, Muramatsu S, et al. Intramuscular injection of AAV-GDNF results in sustained expression of transgenic GDNF, and its delivery to spinal motoneurons by retrograde transport. Neurosci Res 2003;45:33–40.
36. Manabe Y, Nagano I, Gazi MS, et al. Glial cell line-derived neurotrophic factor protein prevents motor neuron loss of transgenic model mice for amyotrophic lateral sclerosis. Neurol Res 2003;25:195–200.
37. Suzuki M, McHugh J, Tork C, et al. GDNF secreting human neural progenitor cells protect dying motor neurons, but not their projection to muscle, in a rat model of familial ALS. PLoS One 2007;2:e689.
38. Thomsen GM, Alkaslasi M, Vit JP, et al. Systemic injection of AAV9-GDNF provides modest functional improvements in the SOD1(G93A) ALS rat but has adverse side effects. Gene Ther 2017;24:245-252.
39. Luz M, Mohr E, Fibiger HC. GDNF-induced cerebellar toxicity: A brief review. Neurotoxicology 2016;52:46–56.
40. Zolotukhin S, Byrne BJ, Mason E, et al. Recombinant adeno-associated virus purification using novel methods improves infectious titer and yield. Gene Ther 1999;6:973–985.
41. Shefner JM, Cudkowicz M, Brown RH, Jr. Motor unit number estimation predicts disease onset and survival in a transgenic mouse model of amyotrophic lateral sclerosis. Muscle Nerve 2006;34:603–607.
42. Homs J, Ariza L, Pages G, et al. Schwann cell targeting via intrasciatic injection of AAV8 as gene therapy strategy for peripheral nerve regeneration. Gene Ther 2011;18:622–630.
43. Modol-Caballero G, Herrando-Grabulosa M, Garcia-Lareu B, et al. Gene therapy for overexpressing Neuregulin 1 type I in skeletal muscles promotes functional improvement in the SOD1(G93A) ALS mice. Neurobiol Dis 2020;137:104793.
44. Nakai H, Herzog RW, Hagstrom JN, et al. Adeno-associated viral vector-mediated gene transfer of human blood coagulation factor IX into mouse liver. Blood 1998;91:4600–4607.
45. Mancuso R, Olivan S, Mancera P, et al. Effect of genetic background on onset and disease progression in the SOD1-G93A model of amyotrophic lateral sclerosis. Amyotroph Lateral Scler 2012;13:302–310.
46. Bromberg MB, Brownell AA. Motor unit number estimation in the assessment of performance and function in motor neuron disease. Phys Med Rehabil Clin N Am 2008;19:509–532,ix.
47. Mitsumoto H, Ulug AM, Pullman SL, et al. Quantitative objective markers for upper and lower motor neuron dysfunction in ALS. Neurology 2007;68:1402–1410.
48. Jing S, Wen D, Yu Y, et al. GDNF-induced activation of the ret protein tyrosine kinase is mediated by GDNFR-alpha, a novel receptor for GDNF. Cell 1996;85:1113–1124.
49. Treanor JJ, Goodman L, de Sauvage F, et al. Characterization of a multicomponent receptor for GDNF. Nature 1996;382:80–83.
50. Sariola H, Saarma M. Novel functions and signalling pathways for GDNF. J Cell Sci 2003;116:3855–3862.
51. Loeb JA, Fischbach GD. Neurotrophic factors increase neuregulin expression in embryonic ventral spinal cord neurons. J Neurosci 1997;17:1416–1424.
52. Loeb JA, Hmadcha A, Fischbach GD, et al. Neuregulin expression at neuromuscular synapses is modulated by synaptic activity and neurotrophic factors. J Neurosci 2002;22:2206–2214.
53. Wang S, Li Y, Paudyal R, et al. Spatio-temporal assessment of the neuroprotective effects of neuregulin-1 on ischemic stroke lesions using MRI. J Neurol Sci 2015;357:28–34.
54. Bohn MC, Connor B, Kozlowski DA, et al. Gene transfer for neuroprotection in animal models of Parkinson's disease and amyotrophic lateral sclerosis. Novartis Found Symp 2000;231:70–89;discussion 89–93.
55. Yamamoto M, Mitsuma N, Inukai A, et al. Expression of GDNF and GDNFR-alpha mRNAs in muscles of patients with motor neuron diseases. Neurochem Res 1999;24:785–790.
56. Li W, Brakefield D, Pan Y, et al. Muscle-derived but not centrally derived transgene GDNF is neuroprotective in G93A-SOD1 mouse model of ALS. Exp Neurol 2007;203:457–471.
57. Guillot S, Azzouz M, Deglon N, et al. Local GDNF expression mediated by lentiviral vector protects facial nerve motoneurons but not spinal motoneurons in SOD1(G93A) transgenic mice. Neurobiol Dis 2004;16:139–149.
58. Suzuki M, McHugh J, Tork C, et al. Direct muscle delivery of GDNF with human mesenchymal stem cells improves motor neuron survival and function in a rat model of familial ALS. Mol Ther 2008;16:2002–2010.
59. Moreno-Igoa M, Calvo AC, Ciriza J, et al. Non-viral gene delivery of the GDNF, either alone or fused to the C-fragment of tetanus toxin protein, prolongs survival in a mouse ALS model. Restor Neurol Neurosci 2012;30:69–80.
60. Yamamoto M, Kobayashi Y, Li M, et al. In vivo gene electroporation of glial cell line-derived neurotrophic factor (GDNF) into skeletal muscle of SOD1 mutant mice. Neurochem Res 2001;26:1201–1207.
61. Song F, Chiang P, Wang J, et al. Aberrant neuregulin 1 signaling in amyotrophic lateral sclerosis. J Neuropathol Exp Neurol 2012;71:104–115.
62. Loeb JA. Neuregulin: an activity-dependent synaptic modulator at the neuromuscular junction. J Neurocytol 2003;32:649–664.
63. Modol-Caballero G, Garcia-Lareu B, Verdes S et al. Therapeutic Role of Neuregulin 1 Type III in SOD1-Linked Amyotrophic Lateral Sclerosis. Neurotherapeutics 2020.
64. Xie F, Zhang F, Min S, et al. Glial cell line-derived neurotrophic factor (GDNF) attenuates the peripheral neuromuscular dysfunction without inhibiting the activation of spinal microglia/monocyte. BMC Geriatr 2018;18:110.
65. Zahavi EE, Ionescu A, Gluska S, et al. A compartmentalized microfluidic neuromuscular co-culture system reveals spatial aspects of GDNF functions. J Cell Sci 2015;128:1241–1252.

Publisher's Note Springer Nature remains neutral with regard to jurisdictional claims in published maps and institutional affiliations.